Bulletin of Electrical Engineering and Informatics
Vol. 15, No. 6, December 2026, pp. 4792~4801
ISSN: 2302-9285, DOI: 10.11591/eei.v15i6.14248

Control of PMSG for a hydroelectric power factory using adaptive sliding mode control with disturbances

Tran Duc Chuyen, Nguyen Thanh Tinh
Faculty of Electrical Engineering-Automation, University of Economics-Technology for Industries, Hanoi, Vietnam

Article Info

Article history:

Received Aug 12, 2026
Revised Sep 10, 2026
Accepted Oct 4, 2026

Keywords:

Adaptive sliding mode control
Disturbance factors
Hydroelectric generator
Intelligent control
Nonlinear control
Turbine permanent magnet synchronous generator

ABSTRACT

This study, calculates, and controls an electric drive system for a hydroelectric generator based on the adaptive sliding mode control (European Green Hydrogen Acceleration Center (EHGASC)) method, with a permanent magnet synchronous generator (PMSG). Here, an integral sliding mode combined with an adaptive law is designed to demonstrate how a fast control response achieves greater convergence than conventional control. An adaptive law is developed to enable the control parameters, especially the switching process, to be quickly and automatically updated online. Therefore, the disturbance affecting the controller can be effectively reduced, and noise, chattering, and nonlinear disturbances can be eliminated using the Sat(.) function for the system. Thus, a perfect control model is created, and the quality of high-speed and low-speed control, as well as angular position control, is consistently satisfactory. The EHGASC system used for the PMSG generator, as proposed by the authors in this paper, demonstrates the advantages of adaptive sliding mode control (ASMC) based on a model. The simulation results presented in the paper show faster performance and more accurate control compared to other control methods. This also forms the basis for the development, design, fabrication, establishment of intelligent controller algorithms for future hydropower plants.

This is an open access article under the CC BY-SA license.

Corresponding Author:

Tran Duc Chuyen
Faculty of Electrical Engineering-Automation, University of Economics-Technology for Industries
Hanoi, Vietnam
Email: tdchuyen@uneti.edu.vn

1. INTRODUCTION

Today, the automation process of some intelligent electric drive systems of machinery, wind turbines, and hydroelectric turbines, has been developing strongly, as shown in Figure 1. This electric drive system always needs to work with high accuracy and limited rotation angle, with minimal damage and safety in all situations (even during strong storms, heavy rain, and sudden changes in floodwaters flowing from upstream). Therefore, to increase the accuracy of controlling the drive system, adaptive sliding-mode control (ASMC) is used to control it by measuring and estimating the current and voltage components in terms of the rotation angle and speed of the motor to evaluate the output components, using an observer to estimate the disturbance, [1]–[5]. From there, the authors went to study the design, calculation, simulation modeling, European Green Hydrogen Acceleration Center (EHGASC), using permanent magnet synchronous generator motor (PMSG) electric motors, taking into account noise, nonlinearity, and uncertainty in the control synthesis, [6]–[9]. From there, in order to improve the control accuracy of the PMSG hydroelectric generator drive system to obtain maximum electrical power, [10]–[13].

Some common control methods use classical (old) controllers for calculation and traditional (not very efficient) controllers such as: using proportional integral derivatives to calculate estimates, fuzzy sliding mode

proportional-derivative (PD), PD method with compensation and combined sliding mode control, PI controller combined with sliding mode control, sliding mode control combined with neural networks, [8], [12]. Furthermore, using adaptive controllers without sliding mode in machining drive systems (not yet resolved), second and third-order linear quadratic regulator (LQR) and many other classical controllers, and recently the authors have also used direct calculation methods, [14]–[19]. In [7], the design, simulation and analysis of PMSG for hydropower plants is based on theory, while in [11] the passive control for small hydropower generation systems using PMSG without using ASMC algorithm for control. In [20], the comparative performance analysis related to the transmission problem from the generator system to the power consumption site is performed; in [21], the multi-objective PMSG hydropower optimization calculation is performed considering water level changes; in [22]–[24], research is conducted on the control strategy of the PMSG-PWM power generation system using tidal energy; in [25], a neural controller is used for predictive control of the hydropower generation system. In addition, many works in Vietnam also study PMSG machines but have not used adaptive sliding mode control. In general, these methods have not yet improved the control quality for the drive system of current hydropower generator turbines [15], [18], [25]. Therefore, it always causes many errors (noise, nonlinear factors) and the system operates inaccurately, resulting in low controller quality. The system works suboptimally, is not synchronized, and is not economically efficient. Therefore, there is a need for a controller that is economically efficient and improves control quality, reducing costs for machinery like EHGASC using PMSG for hydropower plants today, [16], [19], [25].

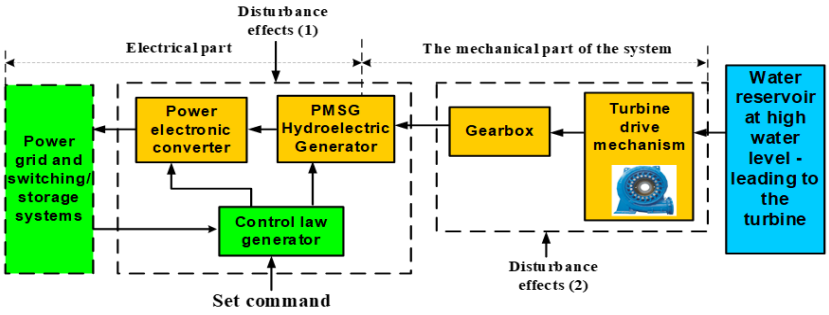


Figure 1. Block diagram of the hydroelectric turbine drive system using PMSG

Figure 1 shows the structure of the PMSG hydroelectric generator drive system. The electrical part includes a power supply, a power electronic converter, a control law generator, and the PMSG generator itself, combined with a speed changer acting as a hydroelectric turbine. The mechanical part includes a speed changer (flexible coupling) connected to the hydroelectric turbine drive mechanism, guiding water flow into the turbine at a certain height. Here, the control law generator used is the ASMC control algorithm, utilizing the PMSG hydroelectric generator.

2. DEVELOPING CONTROL MODELS AND ALGORITHMS FOR EHGASC

2.1. Develop a PMSG control model for EHGASC

The study of EHGASC with the structure introduced in Figure 2. We proceed to study the PMSG hydroelectric generator in vector coordinates with the vector space as shown in Figure 2, [1], [2], [6].

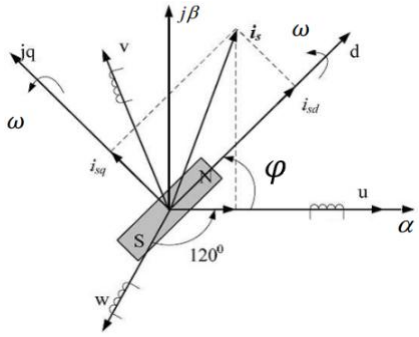


Figure 2. Coordinate system in space of the PMSG hydroelectric generator

Then, take the spatial vector coordinates with the ectangular coordinate d-q system as the reference coordinate system, from which the mathematical model of the PMSG motor is expressed as (1) [1], [2]:

$$\begin{cases} \frac{d\varphi}{dt} = \omega_r \\ \frac{d\omega_r}{dt} = \frac{3\psi_F n_p}{2I} i_q - \frac{\mu}{I}\omega_r - \frac{M_L}{I} \\ \frac{di_d}{dt} = \frac{1}{L_s}(-R_s i_d + n_p \omega_r L_s i_q + v_d) \\ \frac{di_q}{dt} = \frac{1}{L_s}\left(-R_s i_q - n_p \omega_r L_s i_d - n_p \omega_r L_s i_d + v_q\right) \end{cases} \quad (1)$$

In (1), we explain that: the components v_d, v_q are the stator voltage values of the d-axis and q-axis respectively; the current components i_d, i_q are the stator currents of the d-axis and q-axis; L_s is the stator inductance; R_s is the stator resistance; ω_r is the angular velocity of the generator rotor; T_s is the electromagnetic torque; n_p is the number of pole pairs; I is the system moment of inertia; μ is the viscous friction coefficient; M_L is the load torque; and ψ_F is the magnetic flux linkage. Simplifying (1), the motion equation of the PMSG can be obtained as follows: the description of the course of research should be supported references, so the explanation can be accepted scientifically:

$$\frac{d^2\varphi}{dt^2} = \frac{3\psi_F n_p}{2I} i_q - \frac{M_L}{I} = \frac{3\psi_F n_p}{2I} i_q - \frac{\mu\omega_r}{I} + d(t) \quad (2)$$

In which, $d(t) = -\frac{M_L}{I}$ is the disturbance, $d; x_1 = \varphi_r - \varphi;\ \dot{x_1} = x_2;\ x = [x_1, x_2]^T;\ \omega_r$ is the rotor rotation angle, $a = n_p.K_t/J,\ b = -\frac{B}{J}, c(t) = a(i_q(t) - i_q^*(t))$. In reality, the operation of the drive system has disturbance and non-linear factors caused by the load torque T_L .

Assuming the desired position is represented by φ_r and the tracking error is represented by the system state $x_1 = \varphi_r - \varphi$, i_q is defined as the system input u, and $\dot{x_1} = x_2;\ x = [x_1, x_2]^T$; therefore, we have:

$$\dot{x} = \bar{A}x + \bar{B}u - \bar{D}d(t) \quad (3)$$

In there, $\bar{A} = \begin{bmatrix} 0 & 1 \\ 0 & -\frac{\mu}{I} \end{bmatrix}, \bar{B} = \begin{bmatrix} 0 \\ \frac{3\psi_F n_p}{2I} \end{bmatrix}, \bar{D} = \begin{bmatrix} 0 \\ 1 \end{bmatrix}$, is the state matrix.

Using the Euler method for (3), we then have the following discrete model which can be calculated as (4):

$$x(c+1) = (\bar{A}(c) + I)x(c) + T_m \bar{B}u(c) + \bar{C}T_m d(c) \quad (4)$$

In there, the component $x(c) = [x_1(c) \quad x_2(c)]^T$, and T_m the sampling period.

2.2. The ASMC algorithm for PMSG hydroelectric generator system

To address the complexity of PMSG modeling and the difficulty in obtaining an accurate model, a linearized model of the PMSG is used for control. Based on this, the design, calculation, and analysis of a method using an integral sliding surface combined with adaptive laws to achieve high-quality, highly accurate position control for a PMSG for hydroelectric generator are as follows:

With appropriate control $u_m(c)$ so that the output displacement can accurately reach the control target position:

$$y_d(c+1) = F(y_d(c), \dots, y_d(c - N_d), u_m(c), \dots, u_m(c - N_u)) + D_o(c) \quad (5)$$

In this case, $F(.)$ denotes an unknown nonlinear function, N_d and N_u denote the unknown orders of the output and input, and $D_o(c)$ denotes the output noise of the PMSG.

$$y(c+1) = F(y_d(c), \dots, y_d(c - N_d), u_m(c), \dots, u_m(c - N_u)) \quad (6)$$

Replacing (6) with (5) gives us:

$$y_d(c+1) = y(c+1) + D_0(c) \quad (7)$$

Then we have:

$$\nabla y_d(c+1) = \nabla y(c+1) + \nabla D_0(c) \quad (8)$$

In this, we calculate $\nabla y_d(c+1) = y(c+1) - y_d(c), \nabla y_d(c+1) = y(c+1) - y(c)$, and the component $\nabla D_0(c) = D_0(c) - D_0(c-1)$. Therefore, the exact linearization method is chosen to express the relationship between the output shift of the PMSG generator and the control input signal. The following assumptions are satisfied: if the reference $y_r(c+1)$ and the control input $u_m(c)$ are limited, then the output $y_d(c+1)$ always tracking the reference signal. The derivative $y_d(c+1)$ with respect $u_m(c)$ is a continuous function. The control system conforms to the generalized Lipschitz condition. For any time (c) and there exists $|\nabla u_m(c)| \neq 0$ and there exists $|\nabla u_m(c+1)| \leq \eta |\nabla u_m(c)|$, where, $\nabla u_m(c) = u_m(c) = u_m(c-1)$, and η is a constant. A data model defined by tight feedback for PMSG can be written as (9):

$$\nabla y(c+1) = \partial(c) + K)\nabla u_m(c) \quad (9)$$

We substitute (9) into (8) we get:

$$\nabla y_d(c+1) = (\partial(c) + K)\nabla u_m(c) + \nabla D_0(c) \quad (10)$$

The component $\hat{\partial}(c)$ is an estimate of $\partial(c)$, and $\tilde{\partial}(c) = \hat{\partial}(c) - \partial(c)$, then (10) is written:

$$\nabla y_d(c+1) = (\partial(c) + K)\nabla u_m(c) - \tilde{\partial}(c)\nabla u_m(c) + \nabla D_0(c) \quad (11)$$

The disturbance component $D_0(c+1) = -\tilde{\partial}(c)\nabla u_m(c) + \nabla D_0(c)$, then (11) becomes:

$$\nabla y_d(c+1) = (\partial(c) + K)\nabla u_m(c) + D(c) \quad (12)$$

The law for updating the estimated partial derivatives is implemented by considering stability and Lyapunov theory.

$$I\left(\hat{\nabla}(c)\right) = \left\|\nabla y_d(c) - \left(\hat{\partial}(c-1) + K\right)\nabla u_m(c-1) - \hat{D}(c-1)\right\|^2 + w\left\|\hat{\partial}(c) - \hat{\partial}(c-1)\right\|^2 \quad (13)$$

In there, $w > 0$, represents the weighting coefficient, $\hat{D}(c-1)$ is the estimate of $D(c-1)$. Solving the equation to find $\Delta I(\hat{\partial}(c))/\Delta(\hat{\partial}(c)) = 0$ gives the following result:

$$\hat{\partial}(c) = \hat{\partial}(c-1) + \vartheta\left[\nabla y_d(c) - \left(\hat{\partial}(c-1) + K\right)\nabla u_m(c-1) - \hat{D}(c-1)\right]\nabla u_m(c-1)/(w + \nabla u_m(c-1)^2) \quad (14)$$

In which, $0 < \vartheta < 2$ the component $\partial(c)$ is a time-varying parameter, a mechanism for resetting the new parameter is introduced into the parameter estimation algorithm $\left\|\bar{\hat{\partial}}(c)\right\| \leq \bar{\epsilon}, \|\nabla u_m(c-1)\| \leq \epsilon$, hoặc $sign\left(\hat{\partial}(c)\right) \neq sign\left(\hat{\partial}(1)\right)$, and $\hat{\partial}(c) = \hat{\partial}(1)$. The rest, $\hat{\partial}(c)$ is considered according to (14), where $\hat{\partial}(c)$ is the initial value of $\hat{\partial}(c)$.

Calculating the state observer design: Since the total noise $D(c)$ is unknown, the state observer is used to estimate $D(c)$, and $D(c)$ is satisfied. Then, with the following assumptions: for any time step of the parameter update process, $\|\nabla D(c)\| \leq b$, where $\nabla D(c) = D(c) - D(c-1)$ and b is a positive constant. Defining the state variables $H(c) = [y_d(c), D(c)]^T$; the state equation of the system as (15):

$$H(c+1) = AH(c) + B\nabla u(c) + ED(c) \quad (15)$$

In which, $A = \begin{bmatrix} 1 & 1 \\ 0 & 1 \end{bmatrix}, B = \begin{bmatrix} \hat{\partial}(c) + K \\ 0 \end{bmatrix}, E = \begin{bmatrix} 0 \\ 1 \end{bmatrix}$, represents the state matrices in the control. Then, the observer component is written:

$$\hat{H}(c+1) = A\hat{H}(c) + B\nabla u(c) + T_m \mathbb{Z}\left(H(c) - \hat{H}(c)\right) \quad (16)$$

In which, $\hat{H}(k) = \left[\hat{y}_d(c),\ \hat{D}(c)\right]^T$; $\hat{y}_d(c)$ represents the estimated values of $y_d(c)$ and $\mathbb{Z}_0 = [z_1, 0; 0, z_2]$; represents the matrix components of the observer, and $z_1 = 2\sigma_0, z_2 = 2\sigma_0^2$; với σ where σ

is the bandwidth of the observer. With, $\tilde{H}(k) = \left[\tilde{y}_d(c), \tilde{D}(c)\right]^T = \left[y_d(c) - \hat{y}_d(c), D(c) - \hat{D}(c)\right]^T$ is estimation error matrix.

When estimating all state variables, if only the estimation error of the shift $\tilde{y}_d(c)$, is used, the initial sliding mode observer completes the calculation of the value $\hat{y}_d(c)$, and then observes $\hat{D}(c)$. In this case, as $\tilde{y}_d(c)$ decreases, a larger gain value z_{o2} s needed to obtain the estimate of $\hat{D}(c)$.
To solve this problem and improve estimation performance, the observer is constructed as (17) [12]:

$$\hat{H}(c+1) = A\hat{H}(c) + B\nabla u(c) + T_m \mathbb{Z}_0 \left(H(c) - \hat{H}(c)\right) \tag{17}$$

In which, $\mathbb{Z}_0 = [z_{o1}, 0; 0, z_{o2}]$ is the coefficient matrix. During the estimation of $D(c)$ using the observer, we replace $\tilde{y}(c)$ with $\hat{D}(c)$. Combining with (15) and (17), we obtain:

$$\tilde{D}(k) = \tilde{y}_d(c+1) - \tilde{y}_d(c) + T_m z_{o1} \tilde{y}_d(c) \tag{18}$$

Therefore, we define $\nabla\tilde{H}(c+1) = \tilde{H}(c) - \tilde{H}(c-1) = [\nabla\tilde{y}_d(c), \nabla\tilde{D}(c)]$; and the observation error for the observer is given by (19):

$$\frac{1}{T_m}\nabla\tilde{H}(c+1) = \tilde{A}_e\tilde{H}(c) + \tilde{E}_1\frac{\tilde{\partial}(c)\nabla u_m(c)}{T_m} + \tilde{E}_2\frac{\nabla D(c+1)}{T_m} \tag{19}$$

In which, $\tilde{A}_e = \begin{bmatrix} -z_{o1} & \frac{1}{T_m} \\ 0 & -z_{o2} \end{bmatrix}, \tilde{E}_1 = \begin{bmatrix} 1 \\ 0 \end{bmatrix}, \tilde{E}_2 = \begin{bmatrix} 0 \\ 1 \end{bmatrix}$, are the observation matrices. The characteristic polynomial (19) is:

$$P(\gamma) = \gamma^2 + (z_{o1} + z_{o2})\gamma + z_{o1}z_{o2} \tag{20}$$

The gain coefficient of the observer (to increase sensitivity and accuracy in estimating the state, such as the angle-position in a soft drive system) is written as $z_{o1};\ z_{o2}$ must satisfy $T_m\omega_{r0} < 2$.

$$P(\gamma) = (z_{o1} + \gamma)(z_{o2} + \gamma) = (\omega_{r0} + \gamma)^2 \tag{21}$$

Compared to the traditional observer in (16), z_{o2} can be chosen smaller than z_2, which minimizes the peak phenomenon due to excessively high gain. In addition, compared to the traditional observer, the observer of the noise nonlinear components (19) can significantly reduce the phase lag and improve the convergence speed for the system.

With the integral sliding surface chosen by the student and expressions from (11)-(21), representing the relationship between the output component y and the input và đầu vào u. Then we choose the control. $z_{o1} = \omega_{r0}, z_{o2} = \omega_{r0}.\omega_{r0};\ \omega_{r0}T_m < 2$.

$$u_{m\,min} \le u_{m,0}(c) \le u_{mmax} \tag{22}$$

Now we have:

$$\bar{u}_{mmin} \le \frac{u_{m,0}(c) - u_{m,0}(c-1)}{T_m} \le \bar{u}_{mmax} \tag{23}$$

In there, $u_{m\,min}$ and $u_{m\,max}$ respectively represent the lower and upper limits of input signal saturation. $\bar{u}_{mmin}$ and $\bar{u}_{mmax}$ are the saturation speed limits. Therefore, the actual control law is designed as (24):

$$\begin{aligned} u_m(c) &= sat\{u_m(c-1) + \\ &+ sat\left\{\left(u_{m,0}(c) - u_m(c-1)\right), T_m\bar{u}_{mmin}(c), T_m u_{mmax}(c)\right\}, u_{mmin}, u_{mmax}\} \end{aligned} \tag{24}$$

The $sat(.)$ function in adaptive sliding mode control helps limit the control signal, avoiding large oscillations - Chattering caused by sudden changes in the uncertainty function. Then we have:

$$Sat(\Phi, \Phi_{min}, \Phi_{max} = \begin{cases} \Phi_{min}, & \Phi < \Phi_{min} \\ \Phi, & \Phi_{min} \le \Phi \le \Phi_{max} \\ \Phi_{max}, & \Phi > u_{max} \end{cases} \quad (25)$$

In this case, Φ_{max} and Φ_{min} are the upper and lower limits of the $Sat(.)$ function. The problem then is to automatically control the output signal to avoid overload and stabilize the EHGASC system.

$$o(c+1) = \alpha_o o(c) + \left(\hat{\partial}(c) + K\right)(u_{m,o}(c) - u_m(c) \quad (26)$$

with, $\alpha_o \in (0,1), u_{m,0}$ represents the input signal of the system. From (12) and (26), the position output error $e(c+1)$ of the PMSG can be expressed as (27):

$$e(c+1) = y_r(c+1) - y_d(c+1) - o(c+1) = y_r(c+1) - y_d(c) - \alpha_o o(c) - D(c) - \left(\hat{\partial}(c) + K\right).(u_{m,o}(c) - u_m(c-1)) \quad (27)$$

Here we consider the boundary condition that is always positive and discrete with time, and the specified performance function $\eta(c)$ is defined as (28) and (29):

$$-\eta(c) < e(c) < \eta(c) \quad (28)$$

$$\eta(c+1) = \eta_\infty + \varphi_1(\eta(c) - \eta_\infty)(1 - \tanh(\varphi_o c)) \quad (29)$$

Then, we have the structural diagram of the system is presented and described as shown in Figure 3.

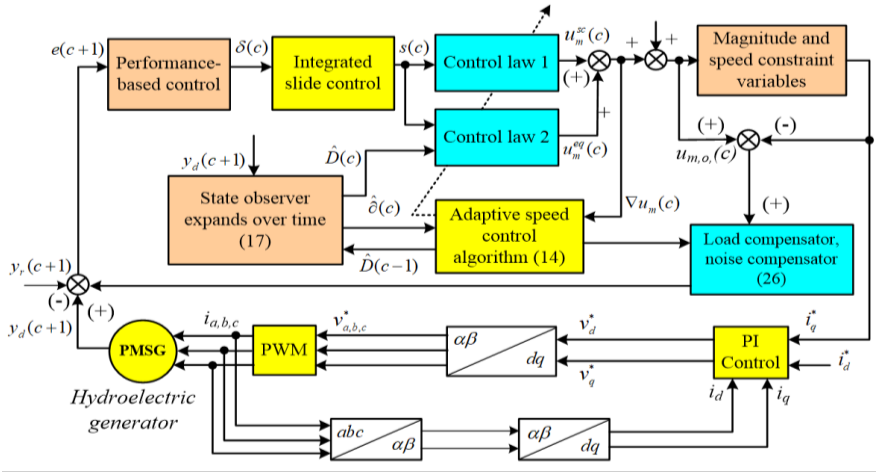


Figure 3. Block diagram of the EHGASC control structure using a PMSG generator

At this point, the definition $\lim_{t\to\infty} \eta(c) = \eta_\infty$; η_0 represents the initial value of $\eta(c)$, satisfying $0 < \eta_\infty < \eta_0$ and the convergence speed φ_1 is the weighting coefficient, representing the rate of decrease of the control function, and φ_0 is the parameter to be designed. Then the problem of controlling the machine's performance as prescribed is always ensured that the position control error remains within the limits predetermined by (28). From this, the convergence of the adaptation law is established under the Lipschitz condition; based on LaSalle's theorem (for autonomous systems) and Lyapunov theory, convergence holds when the system satisfies the aforementioned Lipschitz condition.

In EHGASC system control, the vibration factor, this function can be applied to limit the sensor values, helping to reduce noise and prevent resonance when the oscillation frequency is close to the natural frequency of the control device. With PMSG, applying $Sat(.)$ improves control quality, reduces mechanical noise, and increases the durability of the EHGASC. This function is usually defined as: $Sat(s) = sgn(s)$ if $|s| > \varepsilon$, and $sat(s) = (s/\varepsilon)$ if $|s| \le \varepsilon$, where ε is a small threshold. This helps maintain stability and accuracy

in early fault diagnosis. With $u = -ksat(s/\varepsilon)$, where $sat(s/\varepsilon)$ eliminates abrupt transitions, thus reducing strong chattering while still ensuring convergence to the sliding surface for the EHGASC system.

3. RESULTS AND DISCUSSION

After studying the control algorithm above, we proceed to study the drive control system for the PMSG hydroelectric generator with the following parameters: water head height from 3 m to 15 m with flow rate (0.08-0.15) m³/s, this power of 10 kW. These devices usually operate at a frequency of 50 Hz or 60 Hz, and are certified with quality standards such as ISO9001, CE, and TUV by the Vietnamese electricity industry. Rated torque 16.52 Nm; rated speed=from 250 to 1500 rpm; three phase rectifier; grid-tied PWM inverter; rated efficiency 92%; power factor 6.65×10^{-3} H; 2p=4; torque constant 3.5 bNm/A; link flux 0.4086 Wb; moment of inertia 1.8×10^{-3} kgNm^2; viscous friction constant 9.52×10^{-5} Nm.s/rad; maximum allowable generator speed (max) is 3000 rpm. Parameters were calculated, analyzed (using the Ziegler-Nichols method for calculation), and tuned in MATLAB Simulink with $K_P = 13.5; K_I = 1500$. In addition, to perform simulations with the controller in ASMC mode, there are many other parameters: $\gamma_1 = \gamma_2 = 0.5$; a $= -10$, b $= 10$; $\lambda = 100$; $\beta = 250$; $p = 7$; $q = 1$; $c = 55$; $\alpha_0 = 50$; $\beta(0) = 150$; $\eta(0) = 50$; $k_1 = 0.002$; $k_2 = 0.01$; γ =1.9; $L_d = L_q = 0.126\ H$. From this, we obtain the following simulation results.

In Figure 4, the turbine generator's rotational speed response at 800 rpm at 0.1s during startup shows oscillation. At 0.7 s, the system changes due to disturbances. At 1 s, when the speed changes from 800 rpm to 1200 rpm, the change is negligible. The error response in Figure 5 accurately reflects the operating process. The system's output speed consistently tracks the set speed during generator operation (maximum power output is always achieved).

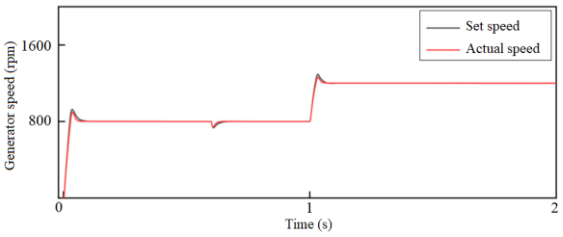


Figure 4. Rotational speed characteristics of the PMSG hydroelectric generator

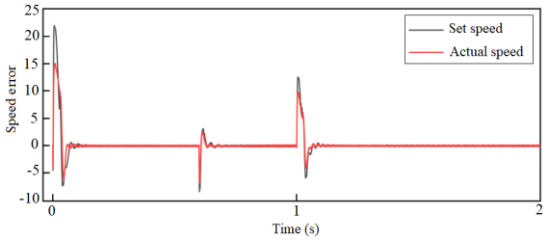


Figure 5. Rotational speed error of the PMSG hydroelectric generator

The simulation with the torque response at varying times at t=1.7 s and t=3.88 s is shown in Figure 6, the actual and estimated rotor control position response values closely tracking the setpoint at each change. In Figure 7, the angular position response (6.3 rad with a total time of 0.5 s) of the EHGASC system requires accurate response when torque changes at different increase/decrease points, while maintaining good system quality. The estimated values of the detector when the machine's position and torque change closely track the input response. The rotor speed of the generator and the estimated speed always closely track the setpoint as shown in Figure 8, and the speed error of the ASMC algorithm always accurately reflects the system value as shown in Figure 9.

In Figure 10, the applied torque curve is the blue line, the estimated response torque curve is the purple line, and the red line represents the electromagnetic torque response of the generator. Initially, the applied torque is 6 Nm, then after 10 seconds it changes to 15 Nm, stabilizing, and after 15 seconds it changes to 12 Nm, stabilizing until 20 seconds. This system exhibits a change when torque is applied. We see that the electromagnetic torque (red line) always closely tracking the set value. The estimated torque at the time of torque change has a delay of 1 second to 3 seconds from the initial set value.

The EHGASC's working response is shown in Figure 11: the purple line represents the input voltage; the red line represents the ASMC response without interference. With a small set angle of 80 degrees, this corresponds to a set angle of 1.39 rad/s (total response time 1s). The purple line represents the preset value, the red line represents the preset response of the sliding mode controller (SMC), and the blue line represents the high-quality ASMC-2 controller response when there is no change in the EHGASC's load torque. In this case, the estimated parameter speed is always accurate, the output closely tracks the input during system balancing,

and the PMSG generator operates stably without errors or static deviations. With the ASMC-1 controller response (the black line represents the ASMC controller response when there is a change in the system's load torque), the EHGASC operates at a speed where the parameter estimation is always accurate (with a change in error compared to ASMC-2). However, the output still closely trackings the input during the balancing process, resulting in stable operation with a small error.

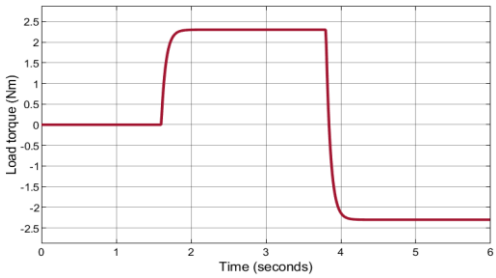


Figure 6. The moment response value represents the load when the PMSG is in operation

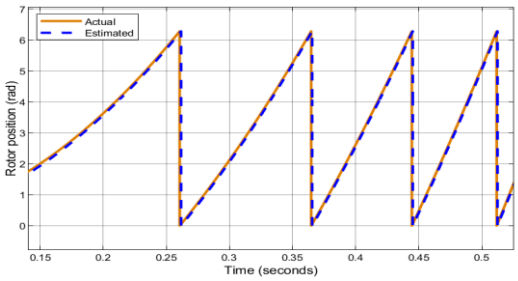


Figure 7. Rotor position response value PMSG

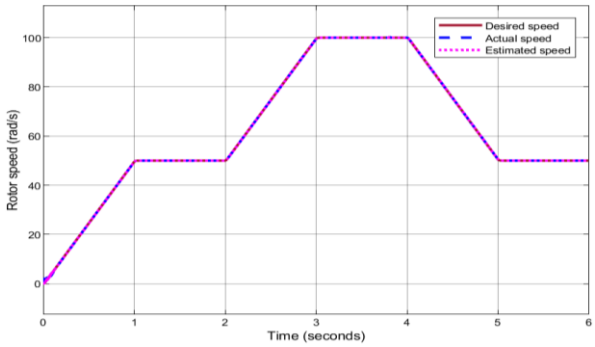


Figure 8. Set speed, actual speed and estimated speed values

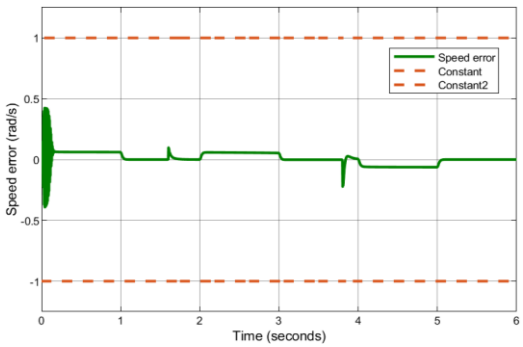


Figure 9. Controller ASMC speed error

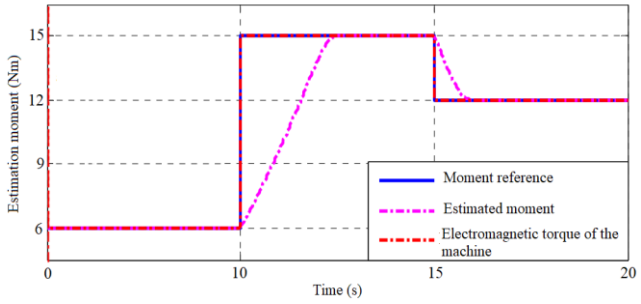


Figure 10. Rotational speed characteristics of the PMSG hydroelectric generator

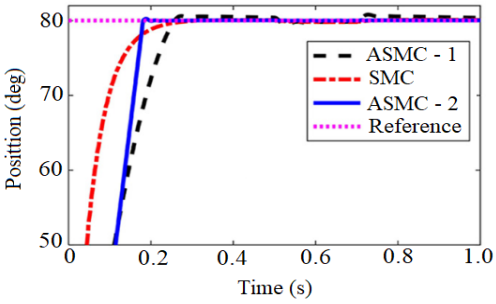


Figure 11. Rotational speed characteristics of the PMSG hydroelectric generator

4. CONCLUSION

From the research results of EHGASC, we see that when equipped with this controller, the PMSG hydroelectric turbine operates with high control quality. The EHGASC output consistently tracking the setpoint during the control process. The estimated speed of the parameters, taking into account disturbances, is always within limits, resulting in high-quality system operation. This demonstrates that the accuracy of the ASMC controller is significantly superior to other methods such as PID, backstepping, simple adaptive control, fuzzy control, neural network control; robust control; or robust adaptive control. Especially for hydroelectric

generators, and wind turbines, the ASMC controller using PMSG, even with disturbances, is always considered optimal and achieves high control quality, maximizing power output for the system/plant. Future development will utilize the EHGASC system in combination with reinforcement learning artificial intelligence (AI) algorithms to enhance system control, resulting in smarter, safer, and more reliable operation of the hydroelectric turbine system.

FUNDING INFORMATION

This research was supported by Faculty of Electrical - Automation; University of Economics-Technology for Industries; No. 218 Hoang Mai Ward, Ha Noi Capital-Vietnam National; http://www.uneti.edu.vn/.

AUTHOR CONTRIBUTIONS STATEMENT

This journal uses the Contributor Roles Taxonomy (CRediT) to recognize individual author contributions, reduce authorship disputes, and facilitate collaboration.

Name of Author	C	M	So	Va	Fo	I	R	D	O	E	Vi	Su	P	Fu
Tran Duc Chuyen	✓	✓	✓	✓	✓	✓	✓	✓	✓	✓	✓		✓	
Nguyen Thanh Tinh		✓		✓		✓		✓	✓	✓	✓	✓		✓

C : **C**onceptualization
M : **M**ethodology
So : **So**ftware
Va : **Va**lidation
Fo : **Fo**rmal analysis
I : **I**nvestigation
R : **R**esources
D : **D**ata Curation
O : Writing - **O**riginal Draft
E : Writing - Review & **E**diting
Vi : **Vi**sualization
Su : **Su**pervision
P : **P**roject administration
Fu : **Fu**nding acquisition

CONFLICT OF INTEREST STATEMENT

Authors state no conflict of interest.

DATA AVAILABILITY

Derived data supporting the findings of this study are available from the corresponding author.

REFERENCES

[1] D. Zholtayev, M. Rubagotti, and T. D. Do, "Adaptive super-twisting sliding mode control for maximum power point tracking of PMSG-based wind energy conversion systems," *Renewable Energy*, vol. 183, pp. 877–889, Jan. 2022, doi: 10.1016/j.renene.2021.11.055.

[2] C. Karasala and S. K. Ganjikunta, "An Adaptive DC-Link Voltage Control of a Multifunctional SPV Grid-Connected VSI for Switching Loss Reduction," *IEEE Transactions on Industrial Electronics*, vol. 69, no. 12, pp. 12946-12956, Dec. 2022, doi: 10.1109/TIE.2021.3128897.

[3] K. Xu, W. Liang, W. Zhao, C. Wang, S. Zou, and X. Zhou, "Vehicle stability and synchronization control of dual-motor steer-by-wire system considering multiple uncertainties," *IEEE Transactions on Transportation Electrification*, vol. 10, no. 2, pp. 3092–3104, Jun. 2024, doi: 10.1109/TTE.2023.3304048.

[4] G. Perozzi, J. J. Rath, C. Sentouh, J. Floris, and J.-C. Popieul, "Lateral shared sliding mode control for lane-keeping assist system in steer-by-wire vehicles: Theory and experiments," *IEEE Transactions on Intelligent Vehicles*, vol. 8, no. 4, pp. 3073–3082, Apr. 2023, doi: 10.1109/TIV.2021.3097352.

[5] G. Yin, R. Wang, and J. Wang, "Robust control for four wheel independently-actuated electric ground vehicles by external yaw-moment generation," *International Journal of Automotive Technology*, vol. 16, no. 5, pp. 839–847, Oct. 2015, doi: 10.1007/s12239-015-0086-2.

[6] J. Baran and A. Jąderko, "An MPPT control of a PMSG-based WECS with disturbance compensation and windspeed estimation," *Energies*, vol. 13, no. 23, Dec. 2020, doi: 10.3390/en13236344.

[7] K. Moodley, S. Maduna, M. Ngongoma, and E. E. Ojo, "Design, simulation, and analysis of PMSG for hydroelectric plant based on the concept of the generalized theory of electrical machines," in *2025 Conference on Information Communications Technology and Society (ICTAS)*, Jul. 2025, pp. 1–6, doi: 10.1109/ICTAS64866.2025.11155541.

[8] L. He, F. Li, C. Guo, B. Gao, J. Lu, and Q. Shi, "An adaptive PI controller by particle swarm optimization for angle tracking of steer-by-wire," *IEEE/ASME Transactions on Mechatronics*, vol. 27, no. 5, pp. 3830–3840, Oct. 2022, doi: 10.1109/TMECH.2021.3137848.

[9] C. D. Sanjenbam and B. Singh, "Predictive control of PMSG-based hydro-electric system with battery supported UPQC," *IEEE Transactions on Consumer Electronics*, vol. 70, no. 1, pp. 238-248, Feb. 2024, doi: 10.1109/TCE.2023.3324509.

[10] M. Fatu, F. Blaabjerg, and I. Boldea, "Grid to standalone transition motion-sensorless dual-inverter control of PMSG with asymmetrical grid voltage sags and harmonics filtering," *IEEE Transactions on Power Electronics*, vol. 29, no. 7, pp. 3463–3472,

Jul. 2014, doi: 10.1109/TPEL.2013.2279883.
[11] W. Gil-Gonzalez, A. Garces, and O. B. Fosso, "Passivity-based control for small hydro-Power generation with PMSG and VSC," *IEEE Access*, vol. 8, pp. 153001–153010, 2020, doi: 10.1109/ACCESS.2020.3018027.
[12] V. Utkin, J. Guldner, and J. Shi, *Sliding mode control in electro-mechanical systems*. CRC Press, 2017, doi: 10.1201/9781420065619.
[13] N. P. Quang and J.-A. Dittrich, *Vector control of three-phase AC machines*. Berlin, Heidelberg: Springer Berlin Heidelberg, 2015, doi: 10.1007/978-3-662-46915-6.
[14] J. Choi, K. Nam, A. A. Bobtsov, and R. Ortega, "Sensorless control of IPMSM based on regression model," *IEEE Transactions on Power Electronics*, vol. 34, no. 9, pp. 9191–9201, Sep. 2019, doi: 10.1109/TPEL.2018.2883303.
[15] P. F. Borowski, "Water and hydropower-challenges for the economy and enterprises in times of climate change in Africa and Europe," *Water*, vol. 14, no. 22, Nov. 2022, doi: 10.3390/w14223631.
[16] A. S. Ghanim and A. N. B. Alsammak, "DQ model of PMSG with the most proficient dynamic analysis in standalone grid," *Journal of Optimization and Decision Making*, vol. 2, no. 1, pp. 199–206, 2023.
[17] R. Sharma, A. Zakerian, and M. K. Ghartemani, "Local controller for an autonomous grid-supportive battery energy storage system," *IEEE Transactions on Power Electronics*, vol. 37, no. 2, pp. 2191–2202, 2021, doi: 10.1109/TPEL.2021.3103539.
[18] R. L. de A. Ribeiro, C. C. de Azevedo, and R. M. de Sousa, "A robust adaptive control strategy of active power filters for power-factor correction, harmonic compensation, and balancing of nonlinear loads," *IEEE Transactions on Power Electronics*, vol. 27, no. 2, pp. 718–730, Feb. 2012, doi: 10.1109/TPEL.2011.2161334.
[19] S. Saberi and B. Rezaie, "Robust adaptive direct speed control of PMSG-based airborne wind energy system using FCS-MPC method," *ISA Transactions*, vol. 131, pp. 43–60, Dec. 2022, doi: 10.1016/j.isatra.2022.04.035.
[20] S. A. O. da Silva, L. B. G. Campanhol, G. M. Pelz, and V. de Souza, "Comparative performance analysis involving a three-phase UPQC operating with conventional and dual/inverted power line conditioning strategies," *IEEE Transactions on Power Electronics*, vol. 35, no. 11, pp. 11652–11665, Nov. 2020, doi: 10.1109/TPEL.2020.2985322.
[21] J. Gao, L. Dai, W. Zhang, and S. Huang, "Multi-objective optimisation of hydroelectric PMSG considering water-level variation," *The Journal of Engineering*, vol. 2019, no. 18, pp. 5234–5239, Jul. 2019, doi: 10.1049/joe.2019.0100.
[22] Y. Ran, M. Qiao, and Y. Xia, "Research on control strategy of PMSG-PWM power generation system with tidal energy," *Electronics*, vol. 13, no. 13, Jun. 2024, doi: 10.3390/electronics13132455.
[23] G. S. Chawda, A. G. Shaik, O. P. Mahela, and S. Padmanaban, "Performance improvement of weak grid-connected wind energy system using FLSRF-controlled DSTATCOM," *IEEE Transactions on Industrial Electronics*, vol. 70, no. 2, pp. 1565–1575, Feb. 2023, doi: 10.1109/TIE.2022.3158012.
[24] A. Gozdowiak and M. Antal, "A synchronization of permanent magnet synchronous generator dedicated for small and medium hydroelectric plants," *Energies*, vol. 18, no. 8, Apr. 2025, doi: 10.3390/en18082128.
[25] M. K.Rajani and M. P.Thanuja, "ANN controller for predictive control of PMSG-based hydro-electric generation with battery-supported UPQC," *Journal of Science Engineering Technology and Management Sciences*, vol. 2, no. 9, pp. 17–33, Sep. 2025, doi: 10.64771/jsetms.2025.v02.i09.pp17-33.

BIOGRAPHIES OF AUTHORS



Tran Duc Chuyen received the Ph.D. degree in Industrial Automation from Le Qui Don Technical University (MTA), Hanoi, Vietnam in 2016; associate professor in 2024. Now, he works at Faculty of Electrical-Automation, University of Economics-Technology for Industries. He works in the Faculty of Electrical-Automations His main researches: electric machine design, electrical machines, drive system, automatic control theory, power electronics and applications, adaptive control, neural network control, robotic control, motion control, microcontrollers and IoT, intelligent control, and artificial intelligence. He can be contacted at email: tdchuyen@uneti.edu.vn.



Nguyen Thanh Tinh was born in Phu Tho Province. He graduated from the University of Electronics and Telecommunications at Hanoi Electric Power University in 2015; and is currently studying for a Master's degree in Electrical Engineering at the University of Industrial Economics and Technology, Vietnam. Currently, he is working at Lai Chau College, Lai Chau Province. His main research fields include: electrical engineering, industrial electronics, power supply systems, electrical and electronic installation; internet of things (IoT), New and renewable energy, adaptive control, sliding control, artificial neural network (ANN) control, and AI. He can be contacted at email: nttinh.24185200004@sv.uneti.edu.vn.